Astron. Astrophys. 355, 17–22 (2000)

ASTRONOMY AND ASTROPHYSICS

Detection of the extra-Galactic background fluctuations at 170 μm*

G. Lagache and J.L. Puget

Institut d'Astrophysique Spatiale, Bât. 121, Université Paris XI, 91405 Orsay Cedex, France

Received 18 March 1999 / Accepted 1 October 1999

Abstract. We have used the Marano1 field observations with ISOPHOT at 170 μm to search for the Cosmic Far-InfraRed Background fluctuations. This field is part of the FIRBACK project (Puget et al. 1999). For the first time, fluctuations due to unresolved extra-Galactic sources are isolated. The emission of such sources clearly dominates, at arcminute scales, the background fluctuations in the lowest Galactic emission regions.

The study presented here is based on a power spectrum analysis which allow to statistically separate each of the background components. With this analysis, we clearly show that we detect the CFIRB fluctuations.

Key words: cosmology: diffuse radiation – infrared: ISM: continuum – infrared: general

1. Introduction

The major component of the extra-Galactic background is formed by the integrated light of all distant galaxies that are not resolved in the beam of the instrument. The detection of the far-infrared part of this background (the CFIRB, Cosmic Far-InfraRed Background) with COBE (Puget et al. 1996; Fixsen et al. 1998; Hauser et al. 1998; Schlegel et al. 1998; Lagache et al. 1999; Lagache et al 2000) has opened new perspectives in our understanding of galaxy evolution. The energy contained in the CFIRB, compared to the one in the UV/optical/near-IR domain (Lagache 1998; Gispert et al. 2000) shows that a new population of galaxies has to be considered in the general framework of galaxy evolution: the far-infrared galaxies. The closest and/or most luminous ones have been discovered by IRAS (see for a review Sanders & Mirabel 1996). Nowadays, the IR galaxies are hunted down by several deep cosmological surveys such as the ones with SCUBA at 850 μm (Hughes et al. 1998; Smail et al. 1997, 1998; Lilly et al. 1999; Barger et al. 1999), ISOPHOT at 170 μm (Kawara et al. 1998; Puget et al. 1999) and ISOCAM at 15 μm (Oliver et al. 1997; Aussel et al. 1999; Désert et al. 1999; Elbaz et al. 1999).

FIRBACK is a deep cosmological survey dedicated to the investigation of the nature of the galaxies that contribute to the CFIRB at 170 μm (Dole et al. 1999) with the ISOPHOT instrument (Lemke et al. 1996). It covers about 4 square degrees. The first FIRBACK field to be observed and analysed is the Marano1 region centered on RA(J2000)=3h13m9.6s and DEC(J2000) = $-$55d03m43.9s. This field covers 0.25 square degree and contains 24 extra-Galactic sources with fluxes ranging from 100 to 850 mJy (Puget et al. 1999). It lies in a very low cirrus emission region with HI column density equal on average to 10^{20} H cm^{-2}. This low cirrus contamination allows to search for brightness fluctuations due to unresolved sources.

In this paper, we use the FIRBACK Marano1 field to isolate the background fluctuations with a high signal to noise ratio. We then discuss the separation of the background fluctuations between the Galactic and extra-Galactic component.

Throughout this paper, "background" refers to the extra-Galactic and Galactic backgrounds, and "CFIRB" to the extra-Galactic background at far-IR wavelengths.

2. Sources of the CFIRB

The CFIRB is made of sources with number counts as a function of flux which can be represented, for the present discussion, by a simple power law:

$$N(>S) = N_0 \left(\frac{S}{S_0}\right)^{-\alpha} \quad (1)$$

For an Euclidean Universe, α=1.5. Obviously, these number counts need to flatten at low fluxes to insure a finite value of the background. Thus, we assume in the present discussion that α=0 for $S < S^*$.

The intensity of the CFIRB, induced by all sources with flux up to S_{max}, is given by:

$$I_{CFIRB} = \int_0^{S_{max}} \frac{dN}{dS} S dS \quad (2)$$

For the simple Euclidean case (α=1.5), the CFIRB integral is dominated by sources near S^*.

Send offprint requests to: G. Lagache (lagache@ias.fr)

* Based on observations with ISO, an ESA project with instruments funded by ESA Member States (especially the PI countries: France, Germany, the Netherlands and the United Kingdom) and with the participation of ISAS and NASA

Fluctuations from sources below the detection limit S_0 (which corresponds to the flux of sources either at the confusion or at the sensitivity limit) are given by:

$$\sigma^2 = \int_0^{S_0} S^2 \frac{dN}{dS} dS \quad \mathrm{Jy}^2/\mathrm{sr} \tag{3}$$

Computing $\frac{dN}{dS}$ using Eq. (1), this gives:

$$\sigma^2 = \frac{\alpha}{2-\alpha} N_0 S_0^2 \left[1 - \left(\frac{S^*}{S_0}\right)^{2-\alpha}\right] \quad \mathrm{Jy}^2/\mathrm{sr} \tag{4}$$

For the simple Euclidean case, the CFIRB fluctuations are dominated by sources which are just below the detection limit S_0.

Nevertheless, it is well known that strong cosmological evolution, associated with a strong negative K-correction, could lead to a very steep number count distribution (see for example Guiderdoni et al. 1998; Franceschini et al. 1998). For $\alpha > 2$, the CFIRB integral is still dominated by sources near S^* but its fluctuations are now also dominated by sources close to S^*. In such a case, observations of the fluctuations will constrain sources that dominate the CFIRB. Furthermore, investigations of problems like the fraction of AGN contributing to the CFIRB, which has been identified as a major question of the coming years, cannot be conducted only with individually detected sources. These observed sources correspond to the bright part of the luminosity function and only represent a few percent of the CFIRB. Moreover, the fraction of AGNs could very well be increasing with luminosity (Sanders & Mirabel 1996). Thus the only way to tackle this problem will be to study the correlation between the extra-Galactic background fluctuations in the X-rays and Far-IR domains.

In the Far-IR, present observations show a very steep slope α=2.2 (Dole et al. 1999). Sources detected above S_0 contribute only to less than 10% of the CFIRB (with S_0=120 mJy). Thus, it is essential to study the extra-Galactic background fluctuations which are likely to be dominated by sources with a flux comparable to those dominating the CFIRB intensity.

3. Summary on the data reduction and calibration

The data reduction and calibration for this field have been detailed in Lagache (1998), Puget et al. (1999) and Puget & Lagache (1999). We are just going to summarise here the different steps.

We use PIA, the ISOPHOT interactive analysis software version 6.4 (Gabriel et al. 1997), to correct for instrumental effects, glitches induced by cosmic particles and to provide an initial calibration. First we apply the non-linearity correction. Deglitching is performed for each individual ramp and then the mean signal per position is derived by averaging the linear fit on each ramp (see Gabriel et al. 1997 for details). The signal shows a long term drift which is corrected by using the two internal calibration (FCS) measurements bracketing each individual observation. Inside each raster, the long term drift represents less than 10% of the signal. The calibration is performed by deriving the mean value of the two FCS measurements. The contribution of the long term drift is thus lower than 5%. Flat fielding is achieved using the high redundancy in the measurements. Glitches inducing long term drifts are also corrected. The flux is finally projected on a $10'' \times 10''$ coordinate grid using our own projection procedure.

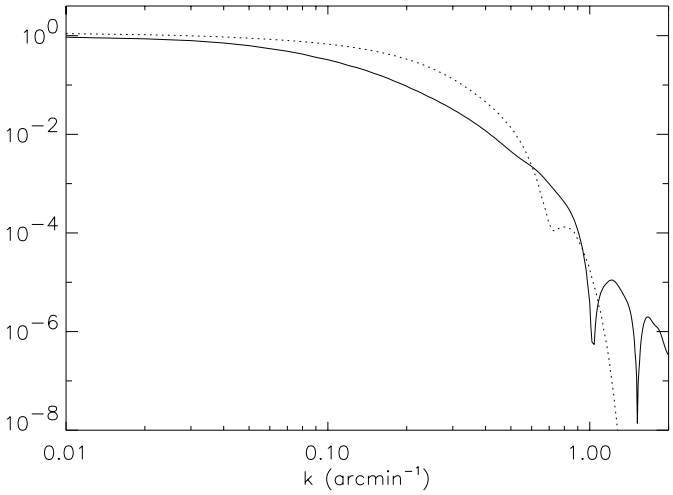

Fig. 1. Continuous line: ISOPHOT Saturn footprint power spectrum (Ws_k). Dotted line: ISOPHOT model footprint power spectrum (Wm_k). The difference in solid angle between the two footprints is equal to 25%.

The final calibration is achieved using the footprint measured on Saturn. It is presented in Fig. 1 of Puget et al. (1999). Brightnesses derived using this footprint are in very good agreement with DIRBE. The footprint measured on Saturn has been compared to the one derived from the diffraction model, including the tripode (Klaas et al. in preparation). The model takes into account the bandpass filter and is computed for a νI_ν=constant spectrum. Thus, comparison between the model and Saturn footprints allows to test the wavelength dependence of the footprint. The solid angle supported by the two footprint differs only by 25%. Comparison of the two footprints power spectra, $\mathrm{Ws_k}$ (Saturn) and $\mathrm{Wm_k}$ (model), is shown on Fig. 1. The Saturn FWHM footprint is quite larger than the model one. The difference between these power spectra will be considered in Sect. 5.2.

The Marano1 observations consist of four 19×19 rasters. Each raster was performed in the spacecraft (Y,Z) coordinate system which is parallel to the edges of the detector array. The field area covered by each raster is about $30' \times 30'$. The exposure time is 16s per pixel. Rasters were performed with one pixel overlap in each Y and Z direction. Therefore, for the maximum redundancy region, the effective exposure time is 256 sec per sky position (16 sec per pixel, 4 rasters and redundancy of 4). Displacements between the four raster centers correspond to 2 pixels. This mode of observation, which does not provide proper sampling of the point-spread-function, was chosen deliberately because it allows a very clean determination of the instrumental noise.

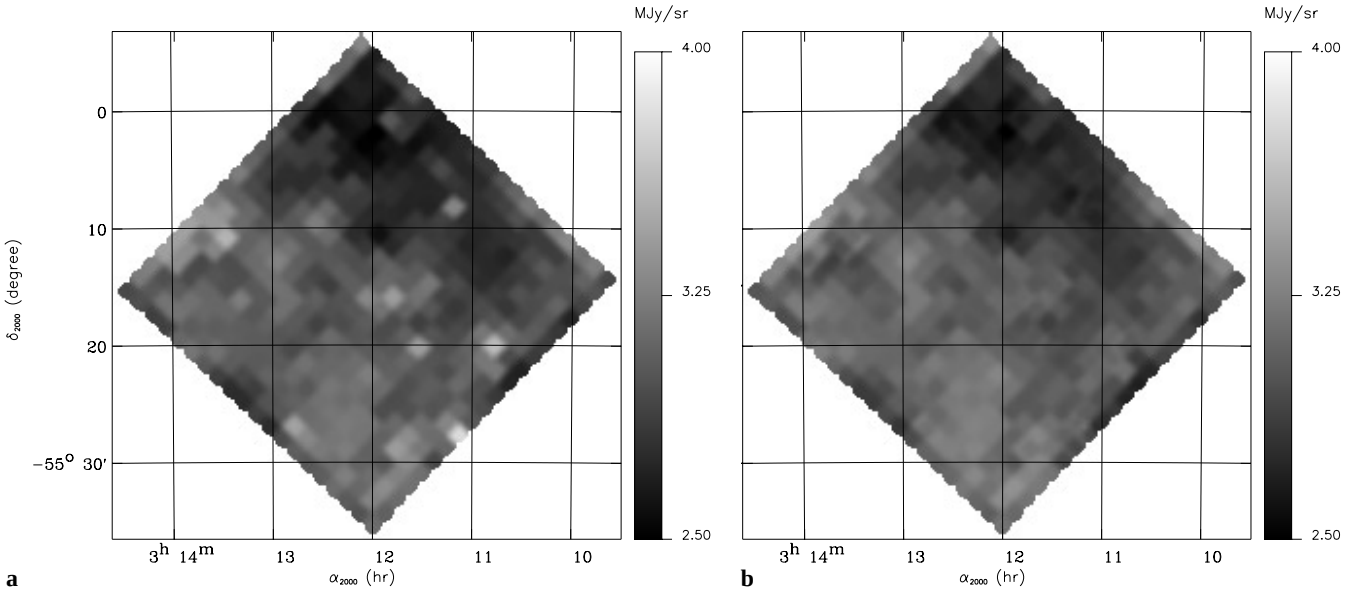

Fig. 2. **a** The Marano1 region observed with ISOPHOT at 170 μm. **b** same as **a** with detected sources removed.

The final map is made of 16 coadded independent maps. The extraction of extra-Galactic sources and determination of their fluxes are made on this final coadded map. To compute the instrumental noise, we have measured the flux of the detected sources on the 16 independent maps. We then compute for each source the standard deviation with respect to the flux measured on the coadded map. The average of all the standard deviations gives the instrumental noise. We obtain 1.74 mJy rms in a $89.4'' \times 89.4''$ pixel. The signal in the map is around 3 MJy/sr. This leads to a very high signal to noise ratio in the map of about 300.

Using the four maps of the Marano1 field presented in Fig. 2 of Puget et al. (1999), we can make an estimate of the instrumental noise power spectrum, making the difference between the independent maps. We know that this power spectrum contains low spatial frequency noise, due to small distorsions in the flat field and slow response changes during the observations. With such map differences, we obtain instrumental noise power spectra for pairs of maps which are all more than 10 times smaller than the measured total flux power spectum (which is presented in Fig. 3). The instrumental noise power spectrum is rather flat in the range k=[0.1, 0.5] arcmin^{-1} (about 30 Jy^2/sr at k$\sim$0.2 arcmin^{-1} and 10 Jy^2/sr at k$\sim$0.4 arcmin^{-1}) and is in very good agreement with the one deduced from the noise (assumed to be white) computed on the extra-Galactic sources (1.74 mJy rms in a $89.4'' \times 89.4''$ pixel). The measured instrumental noise power spectrum is subtracted to the measured power spectrum before the analysis.

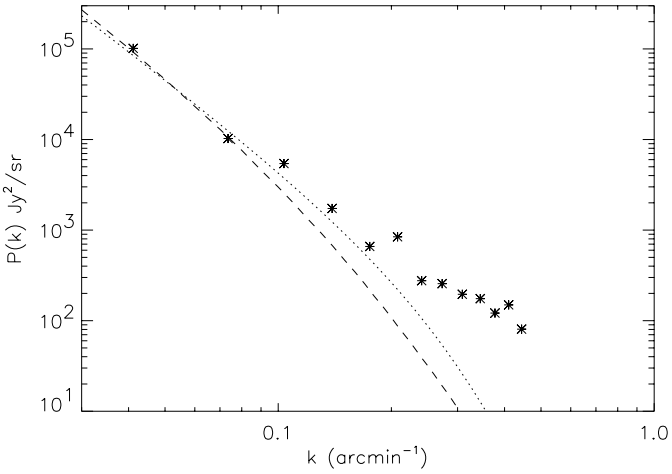

Fig. 3. Power spectrum of the source subtracted map ($*$). The dashed and dotted lines correspond to the cirrus confusion noise multiplied by the footprint power spectrum (Ws_k and Wm_k respectively)

4. The extra-Galactic sources

In the Marano1 field, 24 extra-Galactic sources are detected with fluxes ranging from 100 to 850 mJy (Puget et al. 1999). Sources have been extracted up to the confusion limit (3σ=67.2 mJy) and source fluxes been computed using the Saturn footprint measurement for which a significant fraction of the integral is in the wing (and which is in good agreement with the footprint model). The source subtraction from the Marano1 map is very straightforward. We subtract at each source position the footprint, sampled at 10 arcsec and normalised to unit integral, multiplied by the source flux. The map obtained after the source subtraction is given Fig. 2 together with the original map. The standard deviation in the source subtracted map is around 0.14 MJy/sr, which is very close to the one of the original map which is about 0.15 MJy/sr. For the mean brightness, the difference between the two maps is less than 1%. These numbers clearly show that the background fluctuations are not dominated by strong sources detected above the confusion limit. As for the original map, the source subtracted map has a very high signal to noise ratio.

Background fluctuations (Fig. 2b) are made of two components: the Galactic cirrus one and the extra-Galactic one (the instrumental noise is negligible and is not correlated). We are going now to discuss the relative contribution of these two components.

5. Extra-Galactic and Galactic fluctuation separation

Our separation of the extra-Galactic and Galactic fluctuations is based on a power spectrum decomposition. This method allows us to discriminate the two components using the statistical properties of their spatial behaviour.

We know from previous works that the cirrus far-infrared emission power spectrum has a steep slope in k^{-3} (Gautier et al. 1992; Kogut et al. 1996; Herbstmeier et al. 1998; Wright 1998). These observations cover the relevant spatial frequency range. Furthermore, Abergel et al. (1999) have shown that this spatial structure, measured from extinction, extend to arcsecond scales. Despite a large observational effort, no characteristic scale has been identified in the diffuse interstellar medium (Falgarone 1998).

For the extra-Galactic fluctuations, little is known. The power spectrum of galaxy clustering has been mainly studied from optical surveys. The main result is that the power spectrum can be represented by a simple power law with an index equal to -1.3 at spatial frequency larger than $\sim$0.1 degree^{-1} (Groth & Peebles 1977; Maddox et al. 1990; Peacock 1991; Kashlinsky 1992). For small spatial frequency, if we assume the standard inflationary model (Ω=1 and the Harrison-Zeldovich power spectrum on large scales), the galaxy power spectrum is proportional to k. At Far-IR wavelengths, nothing is known about the galaxy clustering. A spatial and redshift distribution similar to the optical surveys (as the "Automatic Plate Measuring" survey) will give a negative slope around -1.3 whereas a Poissonian distribution will give a flat power spectrum.

In summary, we know that the cirrus emission power spectrum is steep and does not present any characteristic scale. The extra-Galactic component is unknown but certainly much flatter. We thus conclude that the steep spectrum observed in our data at k$<$0.15 arcmin^{-1} (Fig. 3) can only be due to the cirrus emission. The break in the power spectrum at k$\sim$ 0.2 arcmin^{-1} is very unlikely to be due to the cirrus emission itself which is known not to exhibit any preferred scale. Thus, the power spectrum is a powerful tool for a first order separation between the Galactic and extra-Galactic background component. We now give and discuss the quantitative separation of the two components.

5.1. Normalisation of the cirrus emission fluctuations

The cirrus emission has a filamentary structure which, as discussed above, exhibits a spatial power spectrum which has been first determined at 100 μm from IRAS data by Gautier et al. (1992):

$$P_{\mathrm{CC},100}(k) = 1.4 \times 10^{-12} {B_0}^3 \left(\frac{k}{k_0}\right)^{-3} \mathrm{Jy}^2/\mathrm{sr} \qquad (5)$$

with $k_0 = 10^{-2}$ arcmin^{-1}, B_0 the cirrus brightness at 100 μm in Jy/sr and k the spatial frequency in arcmin^{-1}. The main problem in this determination comes from the normalisation which has been established in high cirrus emission regions. This normalisation does not necessarily apply to our very low cirrus emission field. For this reason, the normalisation is directly determined using the measured power spectrum (Fig. 3). Using the low frequency data points and assuming a k^{-3} dependence, we find a power spectum of:

$$P_{\mathrm{CC},170}(k) = 7.9^{+2.1}_{-2.7} \quad k^{-3} \quad \mathrm{Jy}^2/\mathrm{sr} \qquad (6)$$

with k in arcmin^{-1}. The main uncertainty comes from the footprint used for deriving $P_{\mathrm{CC},170}(k)$. The normalisation of the power spectrum derived from the low frequency data points agrees reasonably well with Wright (1998) DIRBE results at high Galactic latitude. It is also in good agreement with the Gautier et al. (1992) normalisation scaled to 170 μm (Appendix A).

5.2. Measured power spectrum

We can now compare the power spectrum measured on the source subtracted map (Fig. 1b) with our estimated one for the non cosmological components defined as:

$$P_{\mathrm{est}} = P_{\mathrm{CC},170} \times W_{\mathrm{k}} \qquad (7)$$

where W_{k} is the ISOPHOT 170 μm beam power spectrum, and $P_{\mathrm{CC},170}$ the cirrus confusion noise. Fig. 3 shows the measured power spectrum together with P_{est} computed for W_{k}=Ws_{k} and W_{k}=Wm_{k} (as defined in Fig. 1). We clearly see an excess between k=0.25 and 0.6 arcmin^{-1} which is more than a factor 10 at k=0.4 arcmin^{-1}. Any reasonable power law spectrum for the cirrus component multiplied by the footprint leads, as can be easily seen in Fig. 3, to a very steep spectrum at spatial frequency k$>$0.2 arcmin^{-1}. This is very different from the observed spectrum. The excess is quite independent of the footprint used. Moreover, it is more than 10 times larger than the measured instrumental noise power spectrum. Therefore, as no other major source of fluctuations is expected at this wavelength, the large excess observed between k=0.25 and 0.6 arcmin^{-1} is interpreted as due to unresolved extra-Galactic sources. The anisotropies of the background are thus dominated, at angular scales close to the angular resolution, by the structure of the CFIRB. This is the first detection of the fluctuations of the CFIRB.

CFIRB fluctuations are clearly detected between k=0.25 and 0.6 arcmin^{-1}. This interval has not enough dynamic range to constrain the slope of the CFIRB fluctuation power spectrum: our present study does not allow to clearly constrain the clustering of galaxies. However, the power spectrum mean level can be determined.

Power spectra with simple power law with index smaller than -1 are not compatible with our measured power spectrum. For indexes in the range [-1,0], the different power laws give equivalent results. For example, on Fig. 4 is shown the total power spectrum obtained by summing up the cirrus confusion noise and a constant CFIRB fluctuation power spectrum,

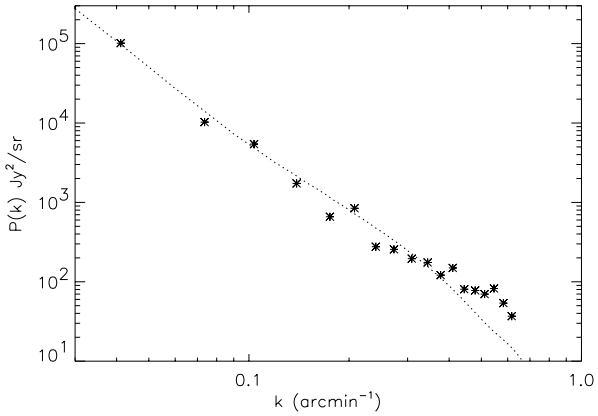

Fig. 4. $*$: power spectrum measured on the map. Dotted line: total power spectra obtained by summing up the cirrus confusion noise (adjusted to our large scale points) and a flat CFIRB fluctuation power spectrum P_{CS} = 7400 Jy^2/sr (we have used here the Saturn footprint power spectrum).

P_{cs} = 7400 Jy^2/sr. This white noise power spectrum level is in very good agreement with the one predicted by Guiderdoni et al. (1997). This gives CFIRB rms fluctuations around 0.07 MJy/sr (for a range of spatial frequency up to 5 arcmin^{-1}). These fluctuations are at the $\sim$9 percent level, which is very close to the predictions of Haiman & Knox (1999).

6. Conclusion

We have shown in the Marano1 region (30′$\times$30′) that the extra-Galactic background fluctuations are well above the instrumental noise and the cirrus confusion noise. The observed power spectrum shows a flattening at high spatial frequencies which is due to extra-Galactic unresolved sources. A preliminary study on the FIRBACK N1 field (2 square degrees) show exactly the same behaviour. The statistical analysis of the background fluctuations using the full FIRBACK fields, covering different high Galactic latitude regions, will allow to constrain models of galaxy evolution and will be a very useful tool for cosmological studies until large passively cooled telescopes in space become available which will allow number counts down to a few mJy. The next step consists of removing the cirrus contribution using gas tracers (the H_α and the 21cm emission lines) to isolate the extra-Galactic fluctuation brightness and thus constrain the clustering of galaxies.

Acknowledgements. We would like to thanks A. Abergel, R. Gispert, F.R. Bouchet for many useful discussions and the ISOPHOT team for many interactions on the data reduction. Thanks to H. Dole for the ISOPHOT footprint model. The work presented here profited from very useful comments from the referee.

Appendix A: comparison of the measured cirrus power spectrum with the Gautier et al. (1992) normalisation

The power spectrum of the cirrus emission derived by Gautier et al. (1992) from IRAS data at 100 μm follows:

$$P_{\mathrm{CC},100}(k) = 1.4 \times 10^{-12} {B_0}^3 \left(\frac{k}{k_0}\right)^{-3} \mathrm{Jy}^2/\mathrm{sr} \qquad \text{(A.1)}$$

with $k_0 = 10^{-2}$ arcmin^{-1}, B_0 the cirrus brightness at 100 μm in Jy/sr and k the spatial frequency in arcmin^{-1}.

The far-infrared Galactic sky at high latitudes has essentially three components: the zodiacal background, the emission from Galactic cirrus and the emission from infrared galaxies at all redshifts. The average total flux in our map is 3.16 MJy/sr. The zodiacal emission has been derived at the time of our observation using the model of Reach et al. (1995) (calibrated on DIRBE data) and is equal to 0.67$\pm$0.07 MJy/sr. Following the DIRBE measurements, the CFIRB at 170 μm is equal to 0.77$\pm$0.25 MJy/sr. Thus, we obtain for the cirrus emission at 170 μm, I(170)=1.72$\pm$0.26 MJy/sr. Using the color ratio for the HI diffuse emission I(170)/I(100)=1.96 (Lagache et al. 1999), we derive B_0= 0.88$\pm$0.13 MJy/sr= 8.8$\pm$1.3 10^5 Jy/sr and the normalisation of the power spectrum at 170 μm becomes:

$$1.4 \times 10^{-12} \left[\frac{I(170)}{I(100)}\right]^2 B_0^3 = 3.63^{+1.9}_{-1.4} \times 10^6 \quad \mathrm{Jy}^2/\mathrm{sr} \qquad \text{(A.2)}$$

Using Eq. (A.1), this gives:

$$P_{\mathrm{CC},170}(k) = 3.63^{+1.9}_{-1.4} \times k^{-3} \quad \mathrm{Jy}^2/\mathrm{sr} \qquad \text{(A.3)}$$

with k in arcmin^{-1}.

In fact Gautier et al. results fit to within a factor of 2 the Eq. (A.1). Taking into account this uncertainty, the cirrus power spectrum becomes:

$$P_{\mathrm{CC},170}(k) = 3.63^{+7.46}_{-2.51} \times k^{-3} \quad \mathrm{Jy}^2/\mathrm{sr} \qquad \text{(A.4)}$$

We do not expect in such a low column density field ($N_{HI} \sim 10^{20}$ H cm^{-2}) any contribution of dust associated with molecular gas (Lagache et al. 1998). Therefore, we can argue that the normalisation of the cirrus confusion noise at 170 μm, for our field, is between 1.1 and 11.1 Jy^2/sr.

Our normalisation computed from the low frequency data points is around 7.9 Jy^2/sr which is in the range of Gautier et al. results. This value of 7.9 Jy^2/sr agree also reasonably well with Wright (1998) measures using DIRBE data.

References

Abergel A., André P., Bacmann A., et al., 1999 In: The Universe as seen by ISO. ESA-SP 427
Aussel H., Cesarsky C.J., Elbaz D., Starck J.L., 1999, A&A in press
Barger A.J., Cowie L.L., Sanders D.B., 1999, ApJ 518, L5
Désert F.X., Puget J.L., Clements D., et al., 1999, A&A in press
Dole H., Lagache G., Puget J.L., et al., 1999, In: The Universe as seen by ISO. ESA-SP 427
Elbaz, D., Cesarsky, C.J., Fadda, D., et al., 1999, A&A 351, 37
Falgarone E., 1998, In: Guiderdoni B., Kembhavi A. (eds.) Starbursts: triggers, nature and evolution. Les Houches School
Fixsen D.J., Dwek E., Mather J.C., et al., 1998, ApJ 508, 123
Franceschini A., Andreani P., Danese L., 1998, MNRAS 296, 709
Gabriel C., Acosta-Pulido J., Henrichsen I., et al., 1997, In: Hunt G., Payne H.E. (eds.) ADAAS VI, ASP Conference series vol. 125, p. 108

Gautier T.N. III, Boulanger F., Pérault M., Puget J.L., 1992, AJ 103, 1313
Gispert R., Lagache, G., Puget, J.L., 2000, A&A submitted
Guiderdoni B., Bouchet B., Puget J.L., et al., 1997, Nat 390, 257
Guiderdoni B., Hivon E., Bouchet F., Maffei B., 1998, MNRAS 295, 877
Groth E.J., Peebles P.J.E., 1977, ApJ 217, 385
Haiman Z., Knox L., 1999, ApJ in press
Hauser M.G., Arendt R.G., Kelsall T., et al., 1998, ApJ 508, 25
Herbstmeier U., Abraham P., Lemke D., et al., 1998, A&A 332, 739
Hughes D.H., Serjeant S., Dunlop J., et al., 1998, Nat 394, 241
Kashlinsky A., 1992, ApJ 399, L1
Kawara K., Sato Y., Matsuhara H., et al., 1998, A&A 336, L9
Kogut A., Banday A.J., Bennett C.L., et al., 1996, ApJ 460, 1
Lagache G., 1998, Ph.D. Thesis, University of Paris XI
Lagache G., Abergel A., Boulanger F., et al., 1998, A&A 333, 709
Lagache G., Abergel A., Boulanger F., et al., 1999, A&A 344, 322
Lagache G., Haffner, L.M., Reynolds, R.J., Tufte, S.L., 2000, A&A 354, 247
Lilly S.J., Eales S.A., Gear W.K.S., et al., 1999, ApJ 518, 641
Lemke D., Klaas U., Abolins J., et al. 1996, A&A 315, L64
Maddox S.J., Efstathiou G., Sutherland W.J., Loveday J., 1990, MNRAS 242, 43
Oliver S.J., Goldschmidt P., Franceschini A., et al., 1997, MNRAS 289, 471
Peacock J.A., 1991, MNRAS 253, 1
Puget J.L., Lagache G., 1999, In: The Universe as seen by ISO. ESA-SP 427
Puget J.L., Abergel A., Bernard J.P., et al., 1996, A&A 308, L5
Puget J.L., Lagache G., Clements D.L., et al., 1999, A&A 354, 29
Reach W.T., Franz B.A., Kelsall T., et al., 1995, In: Dwek E. (ed.) Unveiling the Cosmic Infrared Background. AIP Conf. Proc.
Sanders D.B., Mirabel I.F., 1996, ARA&A 34, 749
Schlegel, D.J., Finkbeiner, D.P., Davis, M., 1998, ApJ 500, 525
Smail I., Ivison R.J., Blain A.W., 1997, ApJ 490, L5
Smail I., Ivison R.J., Blain A.W., Kneib J.P., 1998, ApJ 507, 21
Wright E.L., 1998, ApJ 496, 1